Doc Ophthalmol (2015) 130:111–119
DOI 10.1007/s10633-015-9480-3

ORIGINAL RESEARCH ARTICLE

Rod and cone contributions to the dark-adapted 15-Hz flicker electroretinogram

Jason C. Park · Dingcai Cao · Frederick T. Collison · Gerald A. Fishman · J. Jason McAnany

Received: 20 August 2014 / Accepted: 5 January 2015 / Published online: 13 January 2015

Abstract
Purpose To evaluate rod and cone contributions to the dark-adapted 15-Hz flicker electroretinogram (ERG) across a broad range of stimulus luminances by comparing rod-isolating (ERG_R), cone-isolating (ERG_C), and non-receptor-specific (ERG_{R+C}) responses.
Methods Dark-adapted, full-field 15-Hz ERGs were obtained from four normally sighted subjects (ages 29–36 years) using a four-primary LED-based stimulating system. The primaries were either modulated sinusoidally in phase (ERG_{R+C}) or were modulated in counter-phase to achieve rod isolation (ERG_R) or cone isolation (ERG_C) by means of triple silent substitution. Measurements were made for a broad range of luminances (−2.5 to 1.8 log scot. cd/m^2 in 0.2 log unit steps). Fourier analysis was used to obtain the amplitude and phase of the fundamental response component at each stimulus luminance.
Results Stimulus luminance had different effects on response amplitudes and phases under the three paradigms. Specifically, ERG_C amplitude and phase increased monotonically as luminance increased. The effects on ERG_{R+C} and ERG_R were complex: ERG_{R+C} and ERG_R amplitude was small and the phase decreased for low luminances, whereas amplitude and phase increased sharply at moderate luminances. For high luminances, ERG_{R+C} amplitude and phase increased, whereas ERG_R amplitude decreased and phase was approximately constant.
Conclusions At low luminances, the ERG_{R+C} and ERG_R functions can be attributed to interactions between two rod pathways. At high luminances, the functions can be accounted for by interactions between rod and cone pathways (ERG_{R+C}) or rod insensitivity (ERG_R). The ERG_R paradigm minimizes cone intrusion, permitting assessment of rod function over a large range of luminance levels.

Keywords Electroretinogram (ERG) · Rod · Cone · Flicker

J. C. Park · D. Cao · G. A. Fishman · J. Jason McAnany
Department of Ophthalmology and Visual Sciences, University of Illinois at Chicago, 1855 W. Taylor St., Chicago, IL 60612, USA

D. Cao · J. Jason McAnany
Department of Psychology, University of Illinois at Chicago, 1007 W. Harrison St., Chicago, IL 60612, USA

F. T. Collison · G. A. Fishman
The Pangere Center for Hereditary Retinal Diseases, The Chicago Lighthouse for People Who Are Blind or Visually Impaired, 1850 W. Roosevelt Rd., Chicago, IL 60608, USA

J. Jason McAnany (✉)
Department of Bioengineering, University of Illinois at Chicago, 851 South Morgan St., Chicago, IL 60607, USA
e-mail: jmcana1@uic.edu

Introduction

Electroretinograms (ERGs) elicited by 15-Hz flicker stimuli presented to the dark-adapted eye have been

used to assess the response of the rod pathway across a broad range of luminance levels [e.g. 1–6]. The relationship between the measured response (amplitude and phase) and stimulus luminance is complex. The complex relationship has been attributed to interactions between the cone and rod pathways at mesopic luminance levels and between two different rod pathways at scotopic luminance levels [1]. That is, there is evidence for at least two rod pathways in the mammalian retina [7–14]: a "slow" rod pathway that transmits signals from the rod photoreceptors to rod ON bipolar cells, to AII-amacrine cells, then to cone ON and OFF bipolar cells and subsequently to ganglion cells. A second rod pathway, the "fast" pathway, transmits signals from rod to cone photoreceptors via gap junctions, then to cone ON and OFF bipolar cells and their ganglion cells. The fast and slow rod pathways differ in response timing as well as the luminance range over which they operate, but previous psychophysical [6, 15, 16] and electrophysiological [1–3, 5, 6, 17] work has provided evidence that there is a luminance range over which both pathways operate simultaneously.

For examining how signals from the slow and fast rod pathways interact, 15-Hz flicker stimuli have been particularly useful because this flicker rate maximizes the phase difference between the responses of the two pathways. Specifically, the inter-stimulus interval for 15-Hz flicker is approximately 66 ms and the delay between the two rod pathways is approximately 33 ms, which results in a 180° phase difference between the slow and fast rod pathway responses [5, 16]. If signals with opposite phase are summed vectorially, then cancelation of the summed signal is expected under conditions in which the two pathways produce equal amplitude responses. Indeed, there is evidence that this cancelation occurs in human subjects [5, 6, 15, 16]. For example, as the luminance of a 15-Hz flickering stimulus is increased across the scotopic to mesopic luminance range, the amplitude of the ERG increases, then decreases, before recovering again at higher luminance levels. The loss of ERG amplitude, which is attributed to an interaction between slow and fast rod pathway signals, is referred to as the ERG "15-Hz null" and is associated with a phase change of 180° [4–6, 16].

Although the flicker ERG amplitude null is typically interpreted in the framework of interactions between the slow and fast rod pathways, it is possible that the cone pathway may be involved. Recently, Bijveld et al. [1] evaluated the rod and cone pathway contributions to the 15-Hz flicker ERG null based on differences in rod and cone spectral luminosity sensitivity ($V'(\lambda)$ and $V(\lambda)$, respectively). These investigators reported a 15-Hz flicker ERG null for relatively short wavelength stimuli (465 and 516 nm), but not for longer wavelength stimuli (598 and 638 nm). Based on this result, they concluded that the cone pathway did not contribute to the 15-Hz flicker ERG null. However, the cone pathway is sensitive to all of these wavelengths, so it is difficult to completely rule out cone contributions to the response. Furthermore, the 15-Hz flicker ERG is typically recorded with long trains of flashes, which could affect the subject's state of light adaptation, favoring cone involvement in the response.

For stimuli in the high mesopic luminance range, the role of the cone pathway is more apparent. For these luminance levels, there is an additional rod–cone interaction because there is a phase difference of approximately 180° between the fast rod and cone pathway responses for flicker stimuli near 15 Hz [18]. This phase difference is expected to generate destructive interference, similar to the interaction reported between the fast and slow rod pathways. Consistent with this expectation, previous ERG [18, 19] and psychophysical [20, 21] studies have shown that the combination of rod pathway and cone pathway signals can be described quantitatively by vector summation.

The present study evaluated rod and cone contributions to the dark-adapted 15-Hz ERG across a broad range of luminance levels using a commercially available four-primary photostimulator that was implemented based on the principle of silent substitution [18, 22] to generate three types of temporally modulated stimuli: (1) rod-isolating stimuli in which cone excitation was kept constant (ERG_R), (2) cone-isolating stimuli in which S-, M- and L-cone excitations were modulated in phase while keeping the rod excitation constant (ERG_C), (3) non-receptor-specific stimuli in which both rod and cone excitations were modulated in phase at the same contrast (ERG_{R+C}). The stimuli were modulated sinusoidally, which has the advantage of maintaining constant time-averaged luminance, chromaticity, and state of adaptation. For each stimulus type, the 15-Hz flicker ERG was recorded as a function of luminance level (−2.5 to 1.8 log scot. cd/m^2). In a follow-up experiment, the

15-Hz flicker ERG_{R+C} and ERG_R were recorded in a patient with complete achromatopsia to validate our ability to isolate the rod and cone pathways.

Methods

Subjects

Four male subjects (ages 29, 33, 34, and 36 years) with no history of eye disease, normal color vision (Oculus Heidelberg Multi-Color Anomaloscope), and ETDRS best-corrected visual acuity of 0 log MAR or better (equivalent to 20/20 or better Snellen acuity) participated in the study. Additionally, one 39-year-old female with *CNGB3*-associated achromatopsia was tested in a subset of conditions. The patient has long-standing photoaversion, a lack of color perception, reduced visual acuity of 1.20 log MAR in her tested eye (20/320 Snellen equivalent), and nystagmus. At the age of 5 years, her photopic single-flash ERG was non-detectable, whereas her scotopic single-flash ERG was within normal limits. At the age of 28 years, she matched across the entire range of color mixtures on a Nagel anomaloscope in her tested eye. Informed consent was obtained from all subjects before their participation. Procedures adhered to the tenets of the Declaration of Helsinki, and the protocol was approved by an Institutional Review Board at the University of Illinois at Chicago.

Apparatus and stimuli

Full-field stimuli were generated by a Diagnosys Espion E^2 system and presented in a ColorDome desktop Ganzfeld (Diagnosys LLC, Lowell, MA). Stimuli were the sum of four LED-generated light sources (dominant wavelengths of 465 nm [blue], 515 nm [green], 593 nm [amber] and 642 nm [red]). The approach used to achieve rod- and cone-isolated ERGs is discussed in detail elsewhere [19, 23–25]. In brief, the four LEDs were simultaneously modulated sinusoidally at 15 Hz in phase to achieve combined rod and cone modulation (ERG_{R+C}) or in counter-phase to achieve rod isolation (ERG_R) or cone isolation (ERG_C). The mean luminance (scotopic and photopic cd/m^2), Michelson contrast, and relative phase of each LED are provided in Table 1 for each stimulus paradigm. The luminance values in Table 1 generate stimuli with a mean luminance of 72.5 scotopic cd/m^2 (equivalent to 100 photopic cd/m^2). In all three paradigms, the Michelson contrast of the sine wave stimulus was 40 %, and the chromaticity was constant (CIE 10° coordinates of $x = 0.58$ and $y = 0.40$). Although 50 % contrast could be achieved under the rod-isolating paradigm, the maximum possible contrast under the cone-isolating paradigm was 40 %; consequently, the contrast was set to 40 % under all three paradigms. For the rod-isolating and non-receptor-specific paradigms, the mean luminance of the flicker stimulus spanned a range of over four log units (−2.5 to 1.8 log scot. cd/m^2 equivalent to −2.4 to 1.9 log phot. cd/m^2) in 21 steps spaced approximately 0.2 log units apart. For the cone-isolating paradigm, measurements were made at −0.9 log scot. cd/m^2 (−0.8 log phot. cd/m^2) and from 0.2 to 1.8 log scot. cd/m^2 (0.3 to 1.9 log phot. cd/m^2) in nine steps spaced approximately 0.2 log units apart. Neutral density filters were used to achieve the desired mean luminance levels. Stimulus wavelength and luminance were measured using a Spectrascan 740 (Photo Research, CA).

Procedure and ERG recording

Prior to the monocular ERG recordings, the pupil of the tested eye was dilated with 1 % tropicamide and 2.5 % phenylephrine hydrochloride drops, and the fellow eye was patched. The subject was dark-adapted for 30 min. ERGs were recorded with DTL Plus corneal electrodes, which were referenced to ear clip electrodes, with a gold cup electrode (forehead) serving as ground. Responses were acquired with an Espion E^2 electrophysiology console, with amplifier bandpass settings of 0.30–500 Hz; the sampling frequency was 1 kHz.

ERG recordings for the different paradigms (ERG_{R+C}, ERG_R, ERG_C) were conducted in separate sessions, with the mean luminance level increased sequentially within a session. At each luminance level, 5–10 ERG sweeps were recorded, with a sweep consisting of a 5,016-ms stimulus presentation (76 cycles). The modulation was followed by a dark interval (minimum of 7 s) before the next sweep began. The subjects were alerted by a beep at the beginning of each sweep to minimize eye blinks and movements. Cycles contaminated by eye movement and blink artifacts were removed off-line during the

Table 1 LED parameters for non-receptor-specific and receptor-isolating stimuli

LED peak λ (nm)	Luminance (scot. cd/m^2)	Luminance (phot. cd/m^2)	Non-receptor-specific		Rod-isolating stimulus		Cone-isolating stimulus	
			Contrast	Phase	Contrast	Phase	Contrast	Phase
465	8.58	1.05	0.40	0	0.31	180	0.71	0
515	48.26	16.39	0.40	0	0.80	0	0.40	180
593	14.50	57.62	0.40	0	0.53	180	0.93	0
642	1.12	24.94	0.40	0	0.72	0	0.32	180

data analysis procedure. The time to complete a session was approximately 70 min (rod-isolating and non-receptor-specific paradigms) or 50 min (cone-isolating paradigm). The patient with achromatopsia was tested in one abbreviated session that consisted of fewer luminance steps and fewer sweeps under the rod- and non-receptor-specific paradigms.

Data analysis

The ERG response obtained during the first 1,056 ms of each sweep (16 cycles) was removed to minimize eye movement artifacts and onset transients. The remaining 3,960 ms (60 cycles) of each sweep was divided into six segments of 660 ms (10 cycles), and these six segments were averaged. This procedure was repeated for each of the 5–10 sweeps obtained at each luminance level. A discrete Fourier Transform (DFT), which was implemented in MATLAB using fast Fourier Transform (FFT) algorithms, was performed on each 660-ms waveform to obtain the amplitude and phase of the fundamental component at each mean luminance level for each subject. The phases are given in cosine phase and are "unwrapped" to extend beyond 360°, per convention. A subject's response at a given stimulus luminance was considered statistically distinguishable from noise if the amplitude at 15 Hz was 2.82 times larger than the mean of the noise amplitudes measured at 14 Hz and 16 Hz, which corresponds to a significance value of 0.05, as discussed elsewhere [26].

Results

Figure 1 shows the mean ERG waveforms of the four subjects obtained under each paradigm at three different luminance levels: −0.9, 0.2, and 1.6 log scot. cd/m^2. For clarity, only five cycles are shown and the responses have been bandpass-filtered to remove the high- (>60 Hz) and low-frequency (<5 Hz) noise. The fundamental component of each waveform derived by FFT is represented by the thin gray lines. There was an amplitude increase and leftward shift of the waveforms as mean luminance increased from −0.9 to 0.2 log scot. cd/m^2 under all three paradigms. Further increasing the mean luminance from 0.2 to 1.6 log scot. cd/m^2 increased the ERG_{R+C} (first column) and ERG_C (third column) amplitudes and shifted the waveforms leftward. In contrast, increasing the mean luminance from 0.2 to 1.6 log scot. cd/m^2 decreased the ERG_R amplitude (second column) and had little effect on phase. Thus, the amplitude and phase of the waveforms depended on the stimulus mean luminance, but in different ways under the three paradigms.

Figure 2 shows the mean (±1 SEM) fundamental amplitude (first row) and phase (second row) as a function of stimulus mean luminance for each of the four subjects under the three paradigms. Each subject is represented by a different symbol (given by the key), and data are shown for mean luminance levels greater than −0.9 log scot. cd/m^2, where the SNR was typically greater than the 2.82 criterion that corresponds to a p value of 0.05 [26]. Specifically, SNRs for the ERG_{R+C} (first column) and ERG_C (third column) were >2.82 for all subjects, with the exception of the three lowest luminance levels that were of borderline statistical significance (the SNR for these luminance levels ranged from 1.70 [$p = 0.19$] to 2.34 [$p = 0.09$]). For the ERG_R (second column), the SNRs were >2.82 for the low luminance levels, but were lower for mean luminances above 0.6 log scot. cd/m^2 (SNRs for these luminance levels ranged from 1.67 [$p = 0.20$] to 2.48 [$p = 0.07$]).

Figure 2 shows that ERG_R and ERG_{R+C} amplitude increased sharply between approximately −0.9 and 0

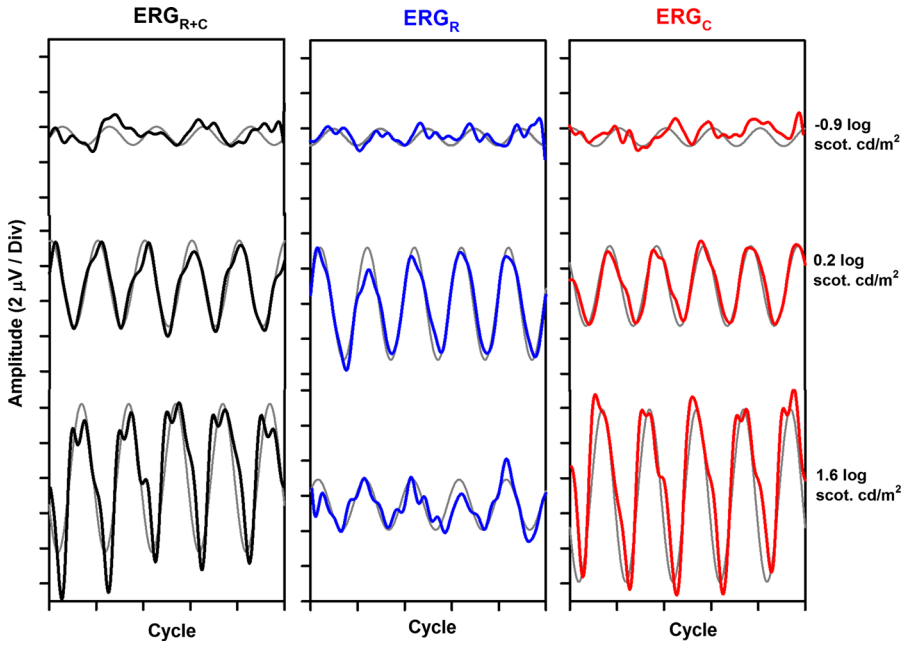

Fig. 1 Example waveforms obtained under the ERG_{R+C} (*first column*), ERG_R (*second column*), and ERG_C (*third column*) paradigms. The waveforms represent the mean of the four subjects obtained at stimulus mean luminance levels of −0.9 (*first row*), 0.2 (*second row*) and 1.6 (*third row*) log scot. cd/m^2. The *thin gray lines* represent the fundamental response component derived by FFT

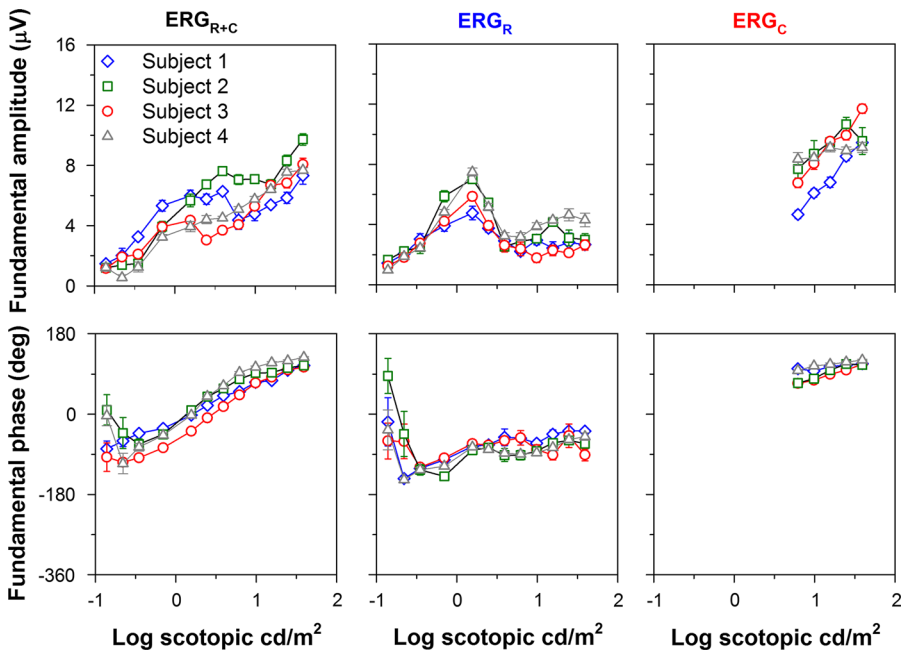

Fig. 2 Mean (±1 SEM) amplitude (*top*) and phase (*bottom*) for each subject as a function of log mean stimulus luminance level obtained under the ERG_{R+C} paradigm (*first column*), ERG_R paradigm (*second column*), and ERG_C paradigm (*third column*)

log scot. cd/m^2. The amplitude functions obtained under the three paradigms differed for stimulus luminance levels greater than approximately 0 log scot. cd/m^2. That is, the ERG_{R+C} amplitude tended to decrease slightly between approximately 0 and 0.6 log scot. cd/m^2, then increase sharply for higher mean luminances. The ERG_R response showed a sharp decrease in amplitude as mean luminance increased from approximately 0 to 0.6 log scot. cd/m^2, followed by a plateau from 0.6 to 1.6 log scot. cd/m^2. The ERG_C response increased approximately monotonically above 0 log scot. cd/m^2 for all four subjects.

The functions relating fundamental phase to stimulus luminance also had complex shapes, consisting of multiple limbs. Phase decreased sharply for ERG_{R+C} and ERG_R between −0.9 and −0.6 log scot. cd/m^2. There was a monotonic phase increase for the ERG_{R+C} function above −0.6 log scot. cd/m^2, whereas the ERG_R function increased monotonically between −0.6 and 0.2 log scot. cd/m^2 and was constant for higher mean luminance levels. ERG_C phase increased slightly as luminance increased over the entire range of luminance levels tested.

Figure 3 permits direct comparison of the ERG_{R+C}, ERG_R, and ERG_C data by plotting the mean amplitudes (upper panel) and phases (lower panel) for the four subjects under the three paradigms (±1 SEM). Data are shown for mean luminance levels greater than −0.9 log scot. cd/m^2, where the mean SNR was >2.82, with the exception of the two lowest luminance levels that were of borderline statistical significance; at −0.9 log scot. cd/m^2 the mean SNR for the ERG_R and ERG_{R+C} was 2.0 ($p = 0.13$), where as the mean SNR was 1.7 ($p = 0.19$) for ERG_C. At −0.7 log scot. cd/m^2, the mean SNR was 2.6 ($p = 0.06$) and 2.4 ($p = 0.08$) for the ERG_R and ERG_{R+C}, respectively.

For the higher luminance levels tested (>0.5 log scot. cd/m^2), the pattern of ERG_{R+C} and ERG_C responses was generally similar in amplitude and phase, suggesting that the ERG_{R+C} was dominated by signals arising from the cone pathway at high luminance levels. However, the ERG_{R+C} amplitude was lower than the ERG_C amplitude across this luminance range. This suggests an interaction between the fast rod pathway and the cone pathway. Specifically, the phase difference between the ERG_R and ERG_C responses was nearly 180°, so a destructive interaction between the responses would be expected. This would result in lower amplitude for the ERG_{R+C} paradigm compared to the ERG_C paradigm, as shown in Fig. 3.

To evaluate quantitatively how ERG_R and ERG_C signals combine, a vector summation model was used to predict the ERG_{R+C} amplitude and phase characteristics. The vector summation model is described in detail elsewhere [18]. In brief, given any two responses (e.g., ERG_R and ERG_C), the third response (ERG_{R+C}) can be estimated by taking into account both the amplitudes and phases of the responses that are being combined. The results of the vector summation model are shown by the solid lines for each of the three paradigms in Fig. 3. The vector

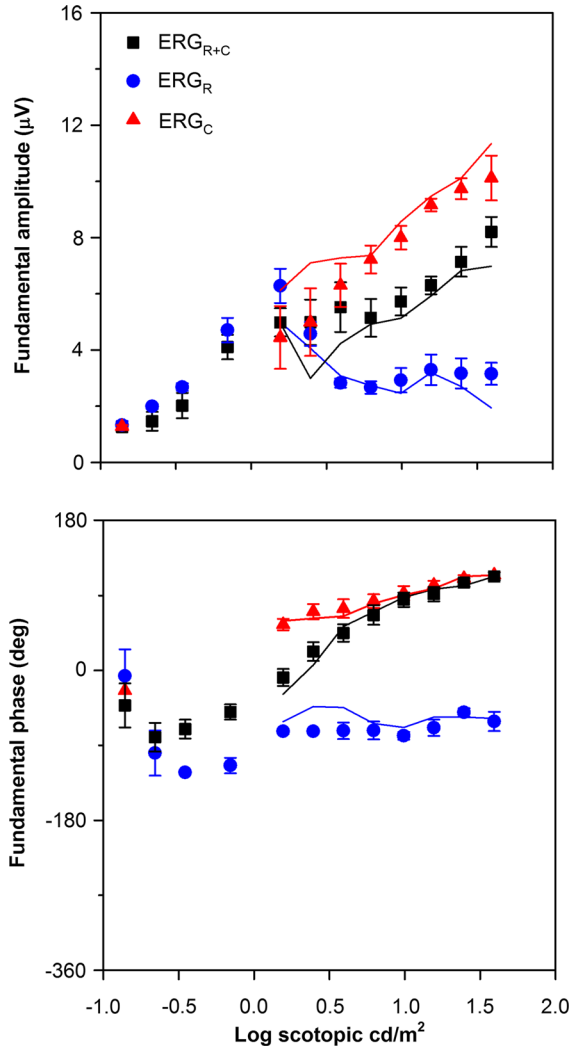

Fig. 3 Mean amplitude (*top*) and phase (*bottom*) of the four subjects (±1 SEM) as a function of log mean stimulus luminance level obtained under the ERG_{R+C} paradigm (*black squares*), ERG_R paradigm (*blue circles*), and ERG_C paradigm (*red triangles*). The *solid lines* represent the results derived from the vector summation model

summation model provided a good description of the amplitude and phase data (mean coefficient of determination, R^2, for the three paradigms was 0.73), providing evidence that the rod and cone responses combine vectorally to yield the ERG_{R+C}. Note that the vectoral subtraction of the ERG_R and ERG_C responses from the ERG_{R+C} response provides a good account of the data (Fig. 3), but there is no known retinal mechanism that would subtract these responses.

In a follow-up experiment, the 15-Hz flicker ERG_{R+C} and ERG_R were recorded in a patient with

complete achromatopsia to validate our ability to isolate the rod and cone pathway responses. The ERG_{R+C} and ERG_R responses of the achromat are expected to be similar, as the patient lacks a cone response. Furthermore, the patient's ERG_{R+C} and ERG_R should approximate the ERG_R of the visually normal subjects shown in Fig. 3. The outcomes of these expectations are shown Fig. 4, which plots the amplitude (top row) and phase (bottom row) of the patient as a function of stimulus mean luminance. The patient's data for the ERG_{R+C} paradigm are shown in the left column (squares), and the middle column shows the patients ERG_R data (circles). The patient's ERG_{R+C} and ERG_R data are replotted together in the right column to facilitate direct comparisons. The gray regions in the left and middle columns represent the range of the normal control data.

The patient's pattern of ERG_{R+C} data (left column) was generally similar to that of the controls for stimulus mean luminances below 1.0 log scot. cd/m^2. However, in marked contrast to the control data, the patient's ERG_{R+C} decreased sharply at 1.0 and 1.6 log scot. cd/m^2. Of note, the patient's ERG_{R+C} phase values (bottom row) were somewhat delayed below 1.0 log scot. cd/m^2 and were delayed by approximately 180° at 1.0 and 1.6 log scot. cd/m^2. The patient's pattern of ERG_R amplitude and phase data (middle column) was generally similar to that of the controls across the entire range of stimulus mean luminance levels tested. The right column of Fig. 4 shows that the patient's pattern of ERG_{R+C} (squares) and ERG_R (circles) amplitude and phase values were similar, as would be expected if the responses were generated by the same pathway.

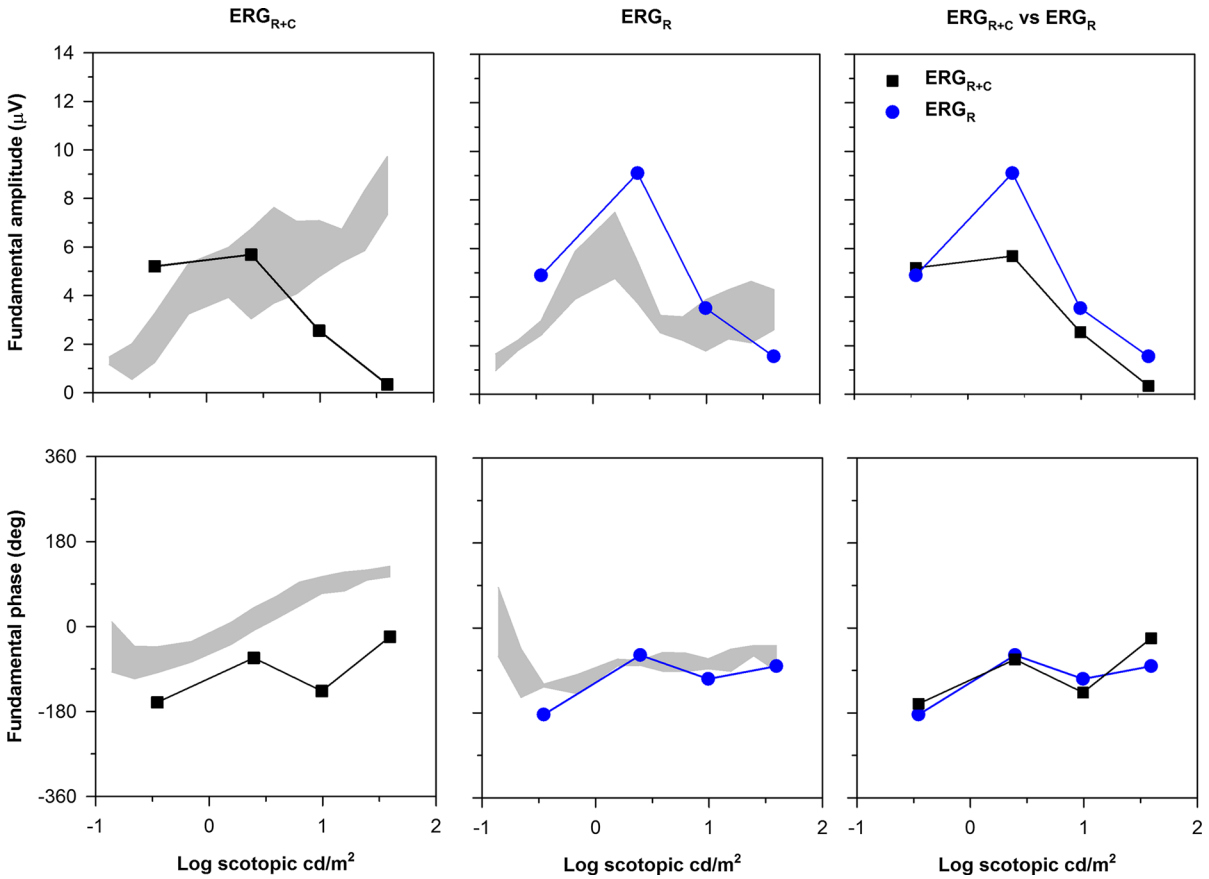

Fig. 4 Amplitude (*top*) and phase (*bottom*) of the patient with achromatopsia (data points and *solid lines*) and the range of normal (minimum and maximum control responses; *gray regions*). Data obtained under the ERG_{R+C} (*first column*) and ERG_R (*second column*) are shown. The *third column* replots the patient's ERG_{R+C} and ERG_R data for direct comparison

Discussion

The purpose of this study was to evaluate the rod and cone contributions to the dark-adapted 15-Hz flicker ERG across a broad range of stimulus luminance levels. The functions relating ERG_{R+C} amplitude and phase to stimulus luminance were complex, consistent with previous findings [1]. The complex shape can be attributed to interactions between the slow and fast rod pathways at low luminance levels, as evidenced by the abrupt phase change, and an interaction between the fast rod pathway and the cone pathway at high luminance levels. The functions relating ERG_R amplitude and phase to stimulus luminance were also complex. The complex shapes can be attributed to interactions between the slow and fast rod pathways at low luminance levels and to the insensitivity of both rod pathways at high luminance levels. Given the similarity of the ERG_{R+C} and ERG_R amplitude and phase functions for low to moderate luminance levels, it appears that the cone pathway has a negligible, or no, involvement in generating the low luminance null and phase change of the ERG_{R+C}, as indicated in previous work [1]. In contrast to the ERG_{R+C} and ERG_R functions, the ERG_C functions were relatively simple; both ERG amplitude and phase increased monotonically over the range of luminance that was assessed.

An additional interaction between the fast rod pathway and the cone pathway is apparent in the ERG_{R+C} responses. This is due to the 180° phase difference between the fast rod and cone pathways, which was also reported by Sharpe and colleagues [16]. The vector summation model provided an excellent account of our rod- and cone-driven ERG responses under all three paradigms. This vector summation model has been shown to be useful for describing rod–cone interactions in previous reports as well [18, 19, 27].

The ERG_R paradigm permits assessment of the integrity of the rod pathways over a large range of luminance levels. This is not possible using standard 15-Hz luminance flicker, because of substantial cone intrusion for moderate to high luminance levels. Rod-driven ERG responses at relatively high luminance (66, 71, and 284 cd/m^2) were also reported in previous silent substitution studies [24, 25], but the present study is the first to map the 15-Hz rod-driven flicker ERG across a broad range of luminance levels. The ability to measure rod function over a broad range of luminance levels without marked cone intrusion may be useful clinically. For example, the ISCEV [28] dark-adapted, single-flash, high luminance (3.0 cd-s/m^2) stimulus, elicits both rod and cone responses (i.e., a "mixed response"), whereas the ERG_R allows high luminance stimuli to be delivered without marked cone intrusion. The use of high luminance stimuli under the ERG_R paradigm may permit rod responses to be better obtained in patients with reduced rod pathway function. Furthermore, it is possible that disease could affect the functional integrity of the fast and slow pathways differently, but further studies are needed to evaluate the extent to which the two pathways are differently susceptible to the effects of disease.

A potential concern in the use of rod- and cone-isolating stimuli is the relative degree of rod and cone isolation. Individual differences in pre-receptoral filtering (principally lens transmittance) may affect the ability to achieve selective rod and cone isolation. However, a previous study using ERG_{R+C}, ERG_R, and ERG_C stimuli in subjects younger than 45 years [18] showed that the impact of isolation error is minimal. The results obtained from the patient with achromatopsia provide additional evidence that effective rod isolation was achieved. Specifically, the pattern of results obtained from the patient with achromatopsia was highly similar to the pattern of results obtained from the visually normal subjects under the ERG_R paradigm. However, the patient with achromatopsia had slightly greater ERG_R amplitudes across the low luminance range compared with the visually normal subjects. Given that data are available from only one patient, it is difficult to determine whether the subtle amplitude difference compared to normal represents the effects of pathology or is simply due to noise and/or individual differences. However, it is of interest to note that a previous study found subtle differences between 15-Hz flicker responses for achromats and visually normal controls, which were suggested to be due to differences in the relative strengths of the slow and fast rod signals [5, 6]. Specifically, the luminance at which the null occurs and the flicker frequency that most clearly generates the ERG null differed slightly between control subjects and a patient who has achromatopsia [5, 6].

In summary, at low luminance levels, the complex shape of the ERG_{R+C} and ERG_R functions can be

attributed to interactions between the slow and fast rod pathways, with negligible (or no) contribution from the cone pathway. At high luminance levels, the shape of ERG_{R+C} function can be accounted for by interactions between the fast rod pathway and the cone pathway, whereas the ERG_R function can be accounted for by rod insensitivity. Thus, the 15-Hz ERG_R paradigm used in the current study permits rod function to be assessed over a wide range of luminance levels by effectively eliminating cone intrusion.

Acknowledgments This research was supported by National Institutes of Health Research Grant R00EY019510 (JM), R01EY019651 (DC), P30EY001792 (core grant), an unrestricted departmental grant from Research to Prevent Blindness, and the Pangere Family Foundation.

Conflict of interest None.

References

1. Bijveld MM, Kappers AM, Riemslag FC, Hoeben FP, Vrijling AC, van Genderen MM (2011) An extended 15 Hz erg protocol (1): the contributions of primary and secondary rod pathways and the cone pathway. Doc Ophthalmol 123(3):149–159
2. Scholl HP, Besch D, Vonthein R, Weber BH, Apfelstedt-Sylla E (2002) Alterations of slow and fast rod erg signals in patients with molecularly confirmed stargardt disease type 1. Investig Ophthalmol Vis Sci 43(4):1248–1256
3. Scholl HP, Langrova H, Weber BH, Zrenner E, Apfelstedt-Sylla E (2001) Clinical electrophysiology of two rod pathways: normative values and clinical application. Graefes Arch Clin Exp Ophthalmol 239(2):71–80
4. Sharpe LT, Stockman A (1999) Rod pathways: the importance of seeing nothing. Trends Neurosci 22(11):497–504
5. Stockman A, Sharpe LT, Ruther K, Nordby K (1995) Two signals in the human rod visual system: a model based on electrophysiological data. Vis Neurosci 12(5):951–970
6. Stockman A, Sharpe LT, Zrenner E, Nordby K (1991) Slow and fast pathways in the human rod visual system: electrophysiology and psychophysics. J Opt Soc Am A 8(10):1657–1665
7. Bloomfield SA, Dacheux RF (2001) Rod vision: pathways and processing in the mammalian retina. Prog Retin Eye Res 20(3):351–384
8. Daw NW, Jensen RJ, Brunken WJ (1990) Rod pathways in mammalian retinae. Trends Neurosci 13(3):110–115
9. Kolb H, Nelson R (1983) Rod pathways in the retina of the cat. Vis Res 23(4):301–312
10. Volgyi B, Deans MR, Paul DL, Bloomfield SA (2004) Convergence and segregation of the multiple rod pathways in mammalian retina. J Neurosci 24(49):11182–11192
11. Wassle H (2004) Parallel processing in the mammalian retina. Nat Rev Neurosci 5(10):747–757
12. Asteriti S, Gargini C, Cangiano L (2014) Mouse rods signal through gap junctions with cones. Elife 3:e01386
13. Dunn FA, Doan T, Sampath AP, Rieke F (2006) Controlling the gain of rod-mediated signals in the mammalian retina. J Neurosci 26(15):3959–3970
14. Robson JG, Maeda H, Saszik SM, Frishman LJ (2004) In vivo studies of signaling in rod pathways of the mouse using the electroretinogram. Vis Res 44(28):3253–3268
15. Conner JD, MacLeod DI (1977) Rod photoreceptors detect rapid flicker. Science 195(4279):698–699
16. Sharpe LT, Stockman A, MacLeod DI (1989) Rod flicker perception: scotopic duality, phase lags and destructive interference. Vis Res 29(11):1539–1559
17. Bijveld MM, Riemslag FC, Kappers AM, Hoeben FP, van Genderen MM (2011) An extended 15 Hz erg protocol (2): data of normal subjects and patients with achromatopsia, csnb1, and csnb2. Doc Ophthalmol 123(3):161–172
18. Cao D, Pokorny J, Grassi MA (2011) Isolated mesopic rod and cone electroretinograms realized with a four-primary method. Doc Ophthalmol 123(1):29–41
19. Kremers J, Scholl HP (2001) Rod-/l-cone and rod-/m-cone interactions in electroretinograms at different temporal frequencies. Vis Neurosci 18(3):339–351
20. MacLeod DI (1972) Rods cancel cones in flicker. Nature 235(5334):173–174
21. van den Berg TJ, Spekreijse H (1977) Interaction between rod and cone signals studied with temporal sine wave stimulation. J Opt Soc Am 67(9):1210–1217
22. Estevez O, Spekreijse H (1982) The "silent substitution" method in visual research. Vis Res 22(6):681–691
23. Cao D, Zele AJ, Pokorny J (2006) Dark-adapted rod suppression of cone flicker detection: evaluation of receptoral and postreceptoral interactions. Vis Neurosci 23(3–4):531–537
24. Kremers J, Pangeni G (2012) Electroretinographic responses to photoreceptor specific sine wave modulation. J Opt Soc Am A Opt Image Sci Vis 29(2):A306–A313
25. Scholl HPN, Kremers J (2001) Electroretinograms in s-cone monochromacy using s-cone and rod isolating stimuli. Color Res Appl 26:S136–S139
26. Meigen T, Bach M (1999) On the statistical significance of electrophysiological steady-state responses. Doc Ophthalmol 98(3):207–232
27. Kremers J, Czop D, Link B (2009) Rod and s-cone driven erg signals at high retinal illuminances. Doc Ophthalmol 118(3):205–216
28. Marmor MF, Fulton AB, Holder GE, Miyake Y, Brigell M, Bach M, International Society for Clinical Electrophysiology of V (2009) Iscev standard for full-field clinical electroretinography (2008 update). Doc Ophthalmol 118(1):69–77